

EXCITATION OF LOW-LEVEL ENERGY WAVE ACCUMULATIONS AND TROPICAL  
CYCLONE FORMATION

A Thesis  
Presented to  
The Academic Faculty

By  
Dana Marie Long

In Partial Fulfillment  
Of the Requirements for the Degree  
Master of Science in the School of  
Earth and Atmospheric Sciences

Georgia Institute of Technology

August 2005

EXCITATION OF LOW-LEVEL ENERGY WAVE ACCUMULATIONS AND TROPICAL  
CYCLONE FORMATION

Approved by:

Dr. Peter Webster, Advisor  
School of Earth and Atmospheric  
Sciences  
*Georgia Institute of Technology*

Dr. Robert Black  
School of Earth and Atmospheric  
Sciences  
*Georgia Institute of Technology*

Dr. Judith Curry  
School of Earth and Atmospheric  
Sciences  
*Georgia Institute of Technology*

Dr. Rong Fu  
School of Earth and Atmospheric  
Sciences  
*Georgia Institute of Technology*

Date Approved: July 15, 2005

I would like to dedicate this to my family. Thank you to my Mom and Dad, my sister Danielle, and my brother David. You all have been my support system and have provided me with much needed prayer and encouragement throughout this two year experience. I would also like to thank all of my friends, especially Dr. Paul Smith, Miss Crystal Gilpin, and Dr. Ray Mooring, who helped to keep me focused and also provided help and encouragement along the way. I would also like to thank Katiá Fernandes, I don't know how I would have made through my first semester without your help. Finally, I would like to thank my creator, for without Him, none of this would be possible.

## ACKNOWLEDGEMENTS

I would first like to thank my thesis advisor, Dr. Peter Webster, for his advice and support. I would also like to thank Dr. Judy Curry, Dr. Robert Black, and Dr. Rong Fu for accepting to be on my thesis reading committee. I would like to give a very sincere and deeply felt thank you to Dr. Hai-Ru Chang for the countless hours of assistance and guidance he provided for me throughout this process. Thank you for your patience. I would also like to thank my group members who provided useful suggestions and assistance throughout my time here at Georgia Tech.

## TABLE OF CONTENTS

Acknowledgements.....	iv
List of Figures .....	vi
Summary .....	viii
Chapter 1 Introduction.....	1
Chapter 2 Tropical Cyclogenesis Theories and Influences.....	3
2.1 Conditional Instability of the Second Kind and Wind-Induced Surface Heat Exchange.....	4
2.2 Modulation of Atlantic Hurricane Activity by the Madden-Julian Oscillation...	6
2.3 Modulation of Eastern North Pacific and Western Pacific Hurricanes by the Madden-Julian Oscillation .....	9
2.4 Energy Wave Accumulation.....	11
2.5 African Easterly Waves and Atlantic Tropical Activity .....	14
Chapter 3 Data and Methodology.....	17
Chapter 4 Results and Discussion .....	29
4.1 Effects of Gaussian Damping.....	30
4.2 Effect of Vorticity Feedback .....	31
4.3 Discussion .....	45
Chapter 5 Conclusion and Future Work .....	47
References.....	49

## LIST OF FIGURES

Figure 2.1 Wind anomalies at 850 mb during (a) westerly MJO phases and (b) easterly MJO phases .....	7
Figure 2.2 Tracks of tropical storms and hurricanes with genesis points in the Atlantic Ocean or Gulf of Mexico during westerly and easterly MJO phases. ....	8
Figure 2.3 Atlantic tropical storm and hurricane positions during (a) westerly and (b) easterly MJO phases .....	9
Figure 2.4 (a) Forward accumulation (b) Backward accumulation.....	12
Figure 2.5 Stretching deformation.....	12
Figure 2.6 Rossby wave accumulation process.....	13
Figure 2.7 Time series showing the interannual variability of the number of AEWs at 850 mb (squares) based on the May–Oct period, together with the number of named storms (stars), hurricanes (triangles), and intense hurricanes (diamonds) as defined by the National Hurricane Center. ....	15
Figure 3.1 MAM a) initial and b) Gaussian damping initial field.....	22
Figure 3.2 JJA a) initial and b) Gaussian damping initial field.....	23
Figure 3.3 SO a) initial and b) Gaussian damping initial field .....	24
Figure 3.4 MAM zonal initial field .....	25
Figure 3.5 JJA zonal initial field .....	25
Figure 3.6 SO zonal initial field .....	26
Figure 3.7 Mean zonal wind at 850 mb during September .....	28
Figure 4.1 SO Zero basic state UVH field without heating (top panel) and with heating (bottom panel) at a) Day 5, b) Day 10, c) Day 15, and d) Day 20 .....	36
Figure 4.2 SO Zonally symmetric basic state UVH field without heating (top panel) and with heating (bottom panel) at a) Day 5, b) Day 10, c) Day 15, and d) Day 20 .....	40

Figure 4.3 SO Zonally symmetric basic state UVH field without heating (top panel) and with heating and vorticity non-feedback region extended (bottom panel) at a) Day 5, b) Day 10, c) Day 15, and d) Day 20 .....	44
---	----

## SUMMARY

A spectral shallow water model is used at the 850 mb level to investigate the effects of cyclonic vorticity on heating in the lower troposphere and how this in turn causes an increase in cyclonic vorticity generation, creating a nonlinear vorticity feedback mechanism.

The model is initialized with NCEP-NCAR reanalysis data from the period 1990-2003 and then used to simulate a heating forcing function centered in east Africa. The model is simulated using a Gaussian damped basic state, a zonally symmetric basic state, and a zero basic state. The heating forcing function is applied to these different basic states with a scaled mass sink to simulate heating in the atmosphere. The heating forcing function creates a vorticity feedback mechanism that increases cyclonic vorticity.

The analysis of these different basic states shows that the Gaussian damped basic state reduces the amplitude of the observational fields at the poles, increases the observational fields in the tropical region and increases the stability of the model at shallow depths. The zero basic state does have a significant effect on cyclonic vorticity generation, but does not improve the capability of the wave to propagate westward into the Atlantic Ocean. The zonally symmetric basic state succeeds in increasing the amount of cyclonic vorticity generated. The zonally symmetric basic state, once the vorticity non-feedback region is extended, is also very effective at increasing the amount of cyclonic vorticity generated and increasing the propagation of this wave westward into the Atlantic Ocean. The analysis suggests that the vorticity feedback mechanism created by the heating forcing function is affected by cyclonic vorticity when a zero and zonally symmetric basic state are used.



# CHAPTER 1

## INTRODUCTION

There are several factors known to be necessary for the formation of tropical cyclones. These include a sea surface temperature warmer than 26.5° C, sufficient planetary vorticity available at latitudes greater than 5° latitude from the equator, low vertical wind shear ( $\partial U/\partial z$ ), the existence of a pre-existing disturbance such as easterly waves, convective instability, and a mid-tropospheric relative humidity high. In addition, there are kinematic influences such as Rossby wave accumulation as an easterly wave moves into regions of negative stretching deformation (e.g.  $\partial U/\partial x < 0$ ) (Webster et al., 2005).

In equatorial regions, the majority of Rossby waves are longitudinally trapped in regions where the stretching of the background flow is negative. As waves propagate and enter a zone of negative stretching deformation, the regions to the east of maximum westerly winds become accumulation zones where the longitudinal wave group speed approaches zero. In the zone of negative stretching deformation, the vorticity and energy density of the waves increase. This leads to strong vertical motion and condensation through frictional convergence (Ekman pumping) in cyclonic regions. The waves also become smaller and more intense. It is hypothesized that this process drives tropical cyclogenesis (Chang and Webster, 1995).

When a wave enters a region of negative stretching deformation, the scale of the wave shrinks longitudinally and stretches latitudinally and cyclonic vorticity increases. It is also hypothesized that this cyclonic vorticity enhances heating in the atmosphere, while anticyclonic vorticity does not. This investigation involves the use of a spectral shallow water model to investigate the effects of a forcing in the form of a heating function that manifests itself as a mass

source/sink. The spectral shallow water model is an atmospheric model that will be used to simulate heating in the atmosphere. The focus of this study will be to show, with the use of this heating function, that cyclonic vorticity enhances heating, and this in turn increases cyclonic activity in the atmosphere from vorticity feedback.

## CHAPTER 2

### TROPICAL CYCLOGENESIS THEORIES AND INFLUENCES

There are two formal theories of tropical cyclogenesis, conditional instability of the second kind (CISK) and wind-induced surface heat exchange (WISHE). The main difference between these two is that with CISK convection drives the large scale circulation and with WISHE convection controls the large scale circulation (Lawrence, 2004).

Many studies have show that the Madden-Julian Oscillation (MJO) modulates tropical cyclone activity in the Atlantic and Pacific Oceans and the Gulf of Mexico. The MJO causes alternating periods of westerly and easterly wind anomalies over the eastern Pacific. Tropical cyclone activity in the Gulf of Mexico appears to vary strongly in association with these wind variations (Maloney and Hartmann, 2000).

Maloney and Hartmann (2000) speculate that the MJO could play a role in regulating tropical cyclone activity in the eastern North Pacific Ocean through variations in meridional shear. Molinari et al. (1997) suggest that MJO wave disturbances and associated shear variations may create periods of instability over the Caribbean Sea and the eastern Pacific through a reversal of the meridional potential vorticity gradient. Cyclogenesis would be favored during these times.

According to Sobel and Bretherton (1999) wave accumulation is an important mechanism in the development of tropical depression type disturbances in the western North Pacific Ocean.

A study conducted by Thorncroft and Hodges (2001) shows that for the period between 1985 and 1998, for the 850-mb level at the West African coast between about 10° and 15°N, there is a notable positive correlation between African Easterly Wave (AEW) activity and

Atlantic tropical cyclone activity. This correlation is particularly strong for the post- European Centre for Medium-Range Weather Forecasts (ECMWF) reanalysis period between 1994 and 1998. This result suggests that Atlantic tropical cyclone activity may be influenced by the number of AEWs leaving the West African coast, which have significant low-level amplitudes, and not simply by the total number of AEWs.

In order to better understand the motivation for this study, I will briefly address the current theories of and some of the factors that influence tropical cyclogenesis.

## 2.1 Conditional Instability of the Second Kind and Wind-Induced Surface Heat Exchange

Conditional instability of the second kind (CISK) is a process whereby low-level convergence in the wind field produces convection and cumulus formation, thereby releasing latent heat. This enhances the convergence and further increases convection (AMS, 2000). With CISK, the pre-hurricane depression and the cumulus cell support one another-the cumulus cell by supplying the heat energy for driving the depression, and the depression by producing low-level convergence of moisture into the cumulus cell (Charney and Eliassen, 1964).

CISK entirely disregards the importance of enhanced heat fluxes from the sea, emphasized by earlier researchers such as Kleinschmidt (1951) and Riehl (1954), and can be shown to rely energetically on stored potential energy in the tropical atmosphere.

The CISK theory suggests that the ocean surface serves as a sink for momentum but not as a source of heat; the spin-up relies on convective energy stored in the atmosphere. This theory is suspect for a variety of reasons. First, careful analyses of the maritime tropical atmosphere show little stored convective energy, and the few locations (such as central North America in spring) that exhibit large amounts of stored convective energy are not known to produce

incipient cyclones. Also, CISK is a fundamentally linear instability; taken at face value, it predicts that incipient cyclones should be ubiquitous features of all convectively unstable atmospheres (Emanuel, 1991).

The second theory for tropical cyclogenesis regards tropical cyclogenesis as resulting from finite-amplitude wind-induced surface heat exchange (WISHE). According to Emanuel (1986), tropical cyclones are developed and maintained against dissipation entirely by self-induced anomalous fluxes of moist enthalpy from the sea surface with virtually no contribution from preexisting convective available potential energy (CAPE). In this sense, the storms are taken to result from an air-sea interaction instability, which requires a finite amplitude initial disturbance. This mechanism involves a positive feedback between the circulation and heat fluxes from the sea surface, with stronger circulation giving rise to larger surface fluxes of heat, which are then quickly redistributed aloft by convection, in turn strengthening the circulation. In this theory, emphasis is placed on the surface fluxes as the principal rate-limiting process; convection serves only to redistribute heat (AMS, 2000).

WISHE modes are regarded as occurring in ambient atmospheres that are neutral to adiabatic displacements of boundary-layer air and hence have no stored convective energy. The re-evaporation of condensed water in the low-entropy air of the middle troposphere appears to be the reason for the finite-amplitude nature of the instability. The resulting downdrafts import low-entropy air into the boundary layer at a rate that exceeds the enthalpy flux from the ocean surface. Intensification occurs when the entropy of the middle-tropospheric air has been raised enough to substantially weaken the low-entropy flux into the boundary layer by downdrafts (Emanuel, 1991).

The CISK hypothesis argues that the interaction between the larger-scale (gradient wind adjustment) and the smaller scale (cumulus convection leading to an unbalanced atmosphere) occurs primarily via the moisture convergence, while WISHE argues that it occurs primarily via increased surface heat and moisture fluxes induced by increased near-surface wind speeds and turbulence (Emanuel, 1991).

According to Craig and Gray (1996), the thing that distinguishes WISHE from CISK is the closure relating convective warming to the intensity of the cyclone vortex, which depends on surface heat and moisture fluxes and does not involve the organizing influence of frictional convergence (Lawrence, 2004).

## 2.2 Modulation of Atlantic Hurricane Activity by the Madden-Julian Oscillation

A positive value of the MJO index coincides with westerly wind anomalies over the eastern Pacific Ocean. Westerly phases are characterized by wind anomalies with cyclonic vorticity over the eastern Pacific and the Gulf of Mexico. Tropical cyclone formation is favored in regions of cyclonic low-level vorticity. MJO easterly phases are characterized by anticyclonic wind anomalies over the eastern Pacific, Gulf of Mexico, and western Caribbean (Maloney and Hartmann, 2000).

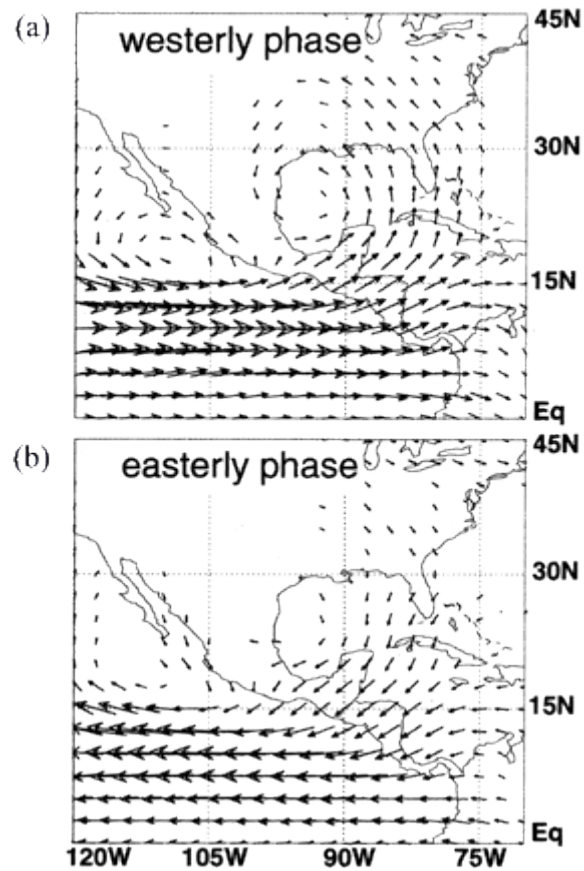


Figure 2.1 Wind anomalies at 850 mb during (a) westerly MJO phases and (b) easterly MJO phases (Maloney and Hartmann, 2000)

The wind pattern in Figure 2.1, showing strongest wind anomalies occurring in the eastern Pacific, is representative of the modulation of eastern Pacific hurricane activity by the MJO. During westerly MJO phases, hurricane genesis in the eastern Pacific is over four times more likely than during easterly periods. Hurricane formation in the eastern Pacific is favored by low-level cyclonic vorticity anomalies, low-level convergence, low vertical wind shear, and the growth of eddy disturbances through barotropic conversion from the mean flow during MJO westerly wind periods (Maloney and Hartmann, 2000).

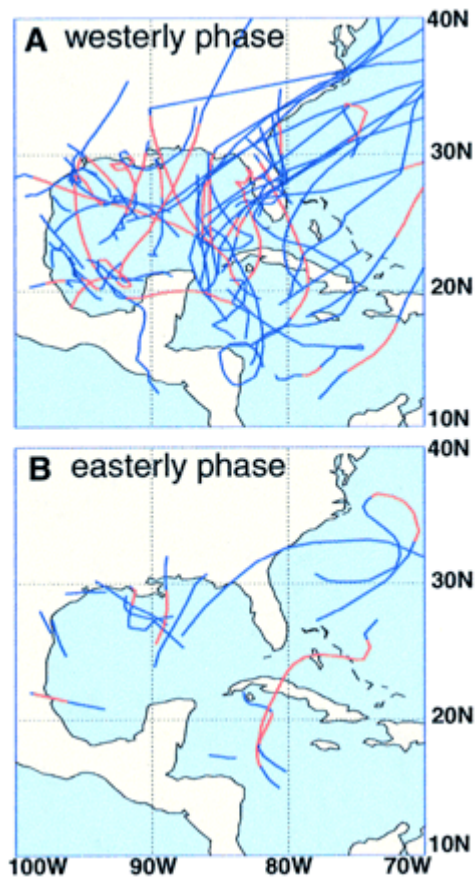


Figure 2.2 Tracks of tropical storms and hurricanes with genesis points in the Atlantic Ocean or Gulf of Mexico during westerly and easterly MJO phases. (Maloney and Hartmann, 2000)

Figure 2.2 show the tracks of tropical storms and hurricanes that developed in the Atlantic Ocean or Gulf of Mexico to the west of  $77.5^{\circ}\text{W}$  during westerly and easterly MJO phases. Tropical cyclone formation during westerly MJO phases outnumber formation during easterly phases by 50 to 14. Hurricane genesis during westerly MJO phases outnumber formation during easterly phases by 24 to 6. The enhancement of tropical cyclone genesis during westerly MJO periods accompanies cyclonic wind anomalies over the Gulf of Mexico and western Caribbean.



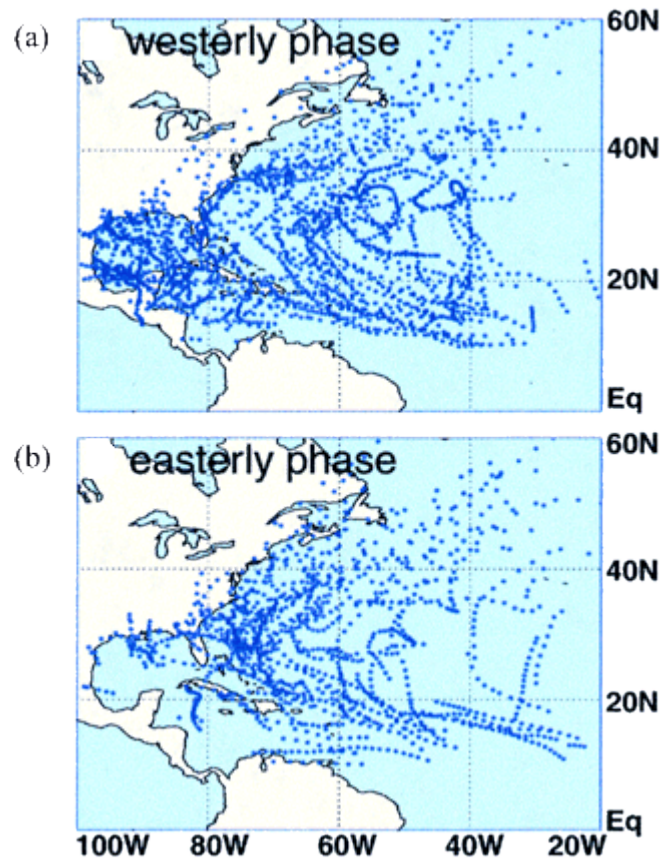


Figure 2.3 Atlantic tropical storm and hurricane positions during (a) westerly and (b) easterly MJO phases (Maloney and Hartmann, 2000)

Figure 2.3 confirms the fact that all tropical cyclone activity is enhanced over the Gulf of Mexico and western Caribbean Sea during westerly MJO events.

### 2.3 Modulation of Eastern North Pacific and Western Pacific Hurricanes by the Madden-Julian Oscillation

Maloney and Hartmann (2000) conclude that a pronounced cycle in the number of named tropical systems in the eastern Pacific Ocean occurs during a composite lifecycle of the MJO. In the eastern Pacific during the composite lifecycle, westerly 850 mb wind anomalies accompany

periods of intensified convection and easterly anomalies accompany suppressed convection. Periods of westerly equatorial 850 mb wind anomalies over the eastern Pacific account for twice as many hurricanes and tropical cyclones as periods of easterly anomalies.

The modulation of hurricane activity over an MJO life cycle can be attributed to changes in environmental conditions in the eastern Pacific. MJO Kelvin waves may influence the large-scale environment over the eastern Pacific hurricane region. Kelvin waves that propagate eastward from western Pacific convective areas enhance convection over the eastern Pacific. Zonal wind anomalies associated with the MJO wave are locally amplified by this anomalous convection. Rossby waves forced by convection and convective inflow over Central America may contribute to the strength of eastern Pacific wind anomalies. Topographic forcing of convection over Central America may be a factor.

The MJO is known to influence western Pacific tropical cyclogenesis (Gray 1979; Yamazaki and Murakami 1989; Liebmann et al. 1994). Liebmann et al. (1994) and Ferreira et al. (1996) have argued that tropical cyclogenesis is favored within the trailing lower-tropospheric equatorial Rossby gyres associated with the MJO convection.

Westerly wind bursts in the western Pacific have a tendency to support tropical cyclone formation because of strong cyclonic shear on the flanks of the equatorial wind anomalies. A similar process might be occurring over the eastern Pacific during certain phases of the MJO. Cyclone intensification can then reinforce wind anomalies toward the equator, creating a positive feedback (Maloney and Hartmann 2000).

## 2.4 Energy Wave Accumulation

In the phenomenon of energy accumulation of transient equatorially trapped modes, regions where the stretching deformation is positive (i.e.  $\partial U/\partial x > 0$ ) are regions of wave action flux (wave energy density) divergence. Regions where  $\partial U/\partial x < 0$  are regions of wave action flux convergence. Thus, the region of convergence occurs to the east of the maximum westerly wind relative to forcing at any location along the equator (Chang and Webster, 1990).

In equatorial regions, the majority of Rossby waves are longitudinally trapped in regions where the stretching deformation of the background flow is negative. Most of the Rossby wave packet will reach the energy accumulation area from the east. This type of wave accumulation is called forward accumulation. Some of the shortwaves of the packet will propagate into the accumulation area from the west. This is known as backward accumulation. According to Chang and Webster (1995) wave accumulation occurs in the vicinity of maximum negative stretching deformation. In the zone of negative stretching deformation, the mode extends latitudinally, shrinks longitudinally, and the group speed decreases. These two concepts are illustrated in Figures 2.4 and 2.5.

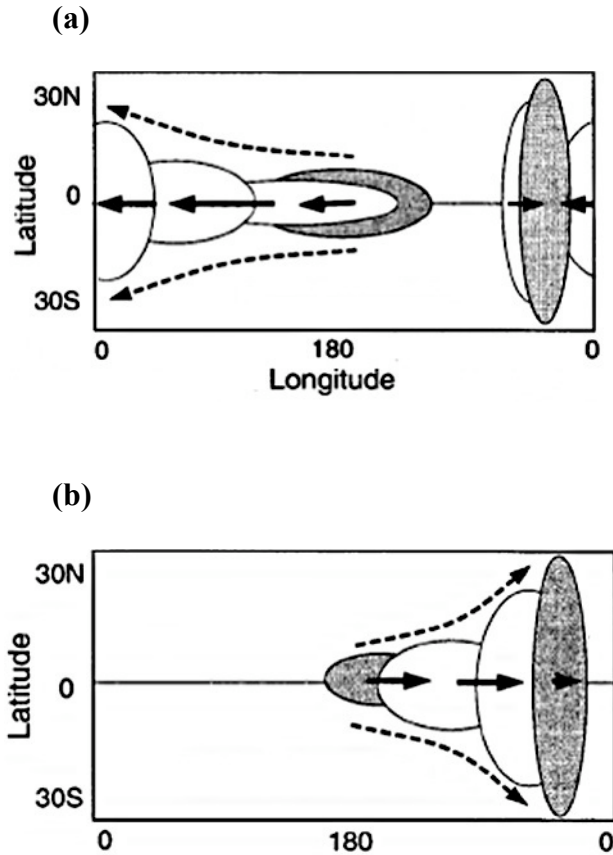


Figure 2.4 (a) Forward accumulation (b) Backward accumulation (Chang and Webster, 1995)

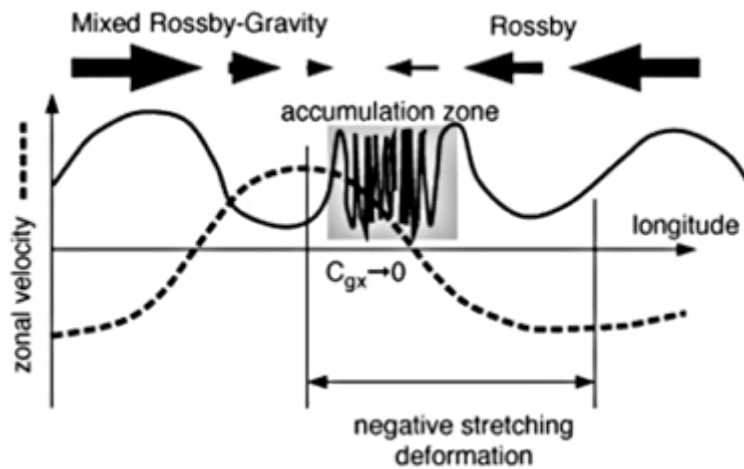


Figure 2.5 Stretching deformation (Webster et al., 2005 85th AMS Meeting)

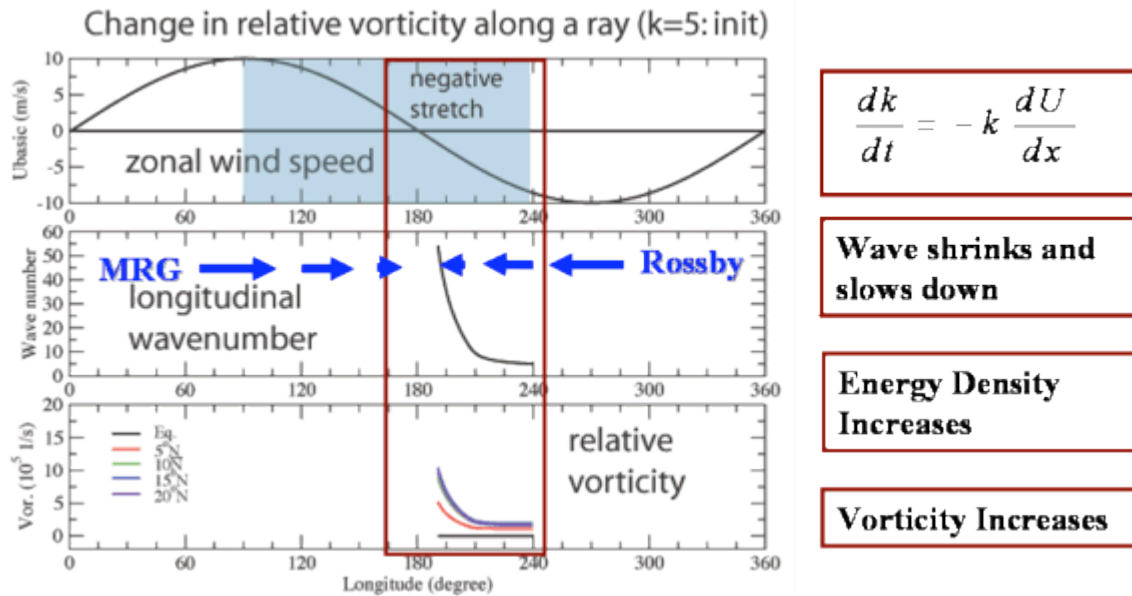


Figure 2.6 Rossby wave accumulation process (Webster et al., 2005)

Figure 2.6 illustrates the process of Rossby wave accumulation. Along a ray, wavenumber,  $k$ , increases and the wave shrinks in regions where easterlies are increasing eastward. Also, along a ray in a  $U=U(x)$  flow, wave energy density will grow in negative stretching regions to conserve wave action flux. This figure also shows that an increase of low-level vorticity may also be one of the necessary conditions for hurricane formation (Webster et al., 2005).

Wave accumulation moves energy to small scales, potentially enhancing, or even driving the tropical cyclone genesis processes (and the opposite for wave decumulation regions) (Webster et al., 2005). According to Sobel and Bretherton (1999), wave accumulation is a promising candidate for the initial development mechanism of tropical depression-type (TD) disturbances.

Sobel and Maloney (2000) found a larger rate of wave accumulation occurs during the convectively active phase than the inactive phase of the MJO. These growing synoptic-scale waves during the active MJO could be the locus of subsequent tropical cyclogenesis.

## 2.5 African Easterly Waves and Atlantic Tropical Activity

Thorncroft and Hodges (2001) proposed that, since an important ingredient of Atlantic tropical cyclogenesis is the presence of finite-amplitude low-level vorticity anomalies, variability in the low-level developments at the West African coast may have an impact on Atlantic tropical cyclone variability. Their analyses of the variability of the 850-mb wave activity at the West African coast showed a peak in the September climatological seasonal cycle consistent with the climatological tropical cyclone activity peak. The interannual variability of the 850-mb wave activity was also compared with the interannual variability of Atlantic tropical cyclone activity. For the period between 1985 and 1998, a notable positive correlation was seen. This suggests that Atlantic tropical cyclone activity may be influenced by the number of AEWs leaving the West African coast, which have significant low-level amplitudes, and not simply by the total number of AEWs.

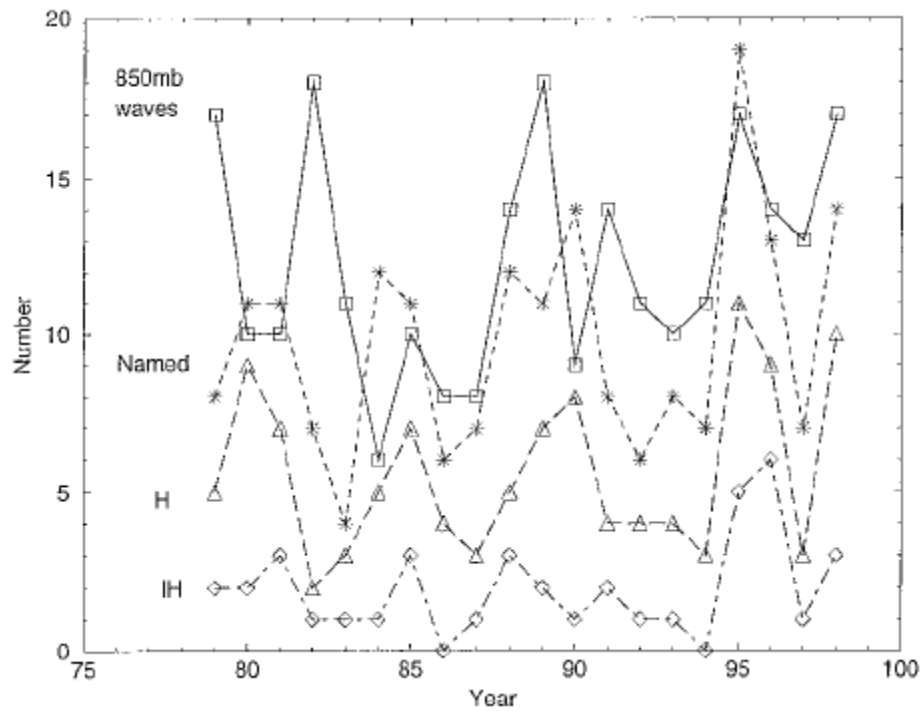


Figure 2.7 Time series showing the interannual variability of the number of AEWs at 850 mb (squares) based on the May–Oct period, together with the number of named storms (stars), hurricanes (triangles), and intense hurricanes (diamonds) as defined by the National Hurricane Center (Thorncroft and Hodges, 2001).

Figure 2.7 shows the correspondence between the AEW activity and tropical cyclone activity. Although, before about 1985 there appears to be a negative correlation between AEW activity at 850 mb and tropical cyclone activity, from 1985 onward there is a strong positive correlation, especially for the post-ECMWF reanalysis period from 1994 to 1998.



## CHAPTER 3

### DATA AND METHODOLOGY

This study involves the use of a spectral shallow water model to investigate the effects of a heating function on cyclonic vorticity generation. The shallow water equations provide a framework for the analysis of the dynamics of large-scale atmospheric flow. The global shallow water equation model used in this study is based on the spectral transform method, thus the name spectral shallow water model (SSWM) (Hack and Jakob, 1992).

The datasets used in this study include zonal and meridional wind and geopotential height data from The National Centers for Environmental Prediction - National Center for Atmospheric Research (NCEP-NCAR) reanalysis, (Kalnay et al. 1996) for the period from 1990 to 2003. The data was used for model initialization.

The SSWM has a horizontal resolution of triangular spectral truncation at wave number 36 (which was transformed into a grid of 60 longitude points and 144 latitude points) and a temporal resolution of 450 seconds. There is no vertical resolution in the model and it consists of only one level. The level the model was simulated at was 850 mb. This level was chosen because it is hypothesized that hurricanes develop in the lower troposphere (Webster et.al, 2005) and the 850 mb wind field represents the lower tropospheric wind field. Using the 850 mb wind field will allow us to look at divergent modes in the lower troposphere.

Using the example of a three dimensional stratified model of the atmosphere, there are two parts to the solution of this model, a vertical part and a horizontal part. Assuming a linear system and that the coefficients of the equations are simple, the three dimensional equation can be separated into a vertical equation and a horizontal equation. The separation constant for the

vertical and horizontal equations is the equivalent depth. The horizontal equation is two dimensional, consisting of latitude and longitude, and is the basis for the shallow water model.

The SSWM was chosen for this study because it is able to model a fluid having a shallow equivalent depth. This depth comes from the vertical structure of the atmosphere and deals with the depth of the heating. Deep heating, occupying the entire troposphere, may have a large equivalent depth, for example 1000 - 1500 m. Shallow heating may have a smaller equivalent depth such as 100 - 500 m. In the context of this study, we are using an equivalent depth of 250 m, which is shallow heating. The SSWM does not include or use sea surface temperature data and does not consider sea surface temperature in its simulations.

The SSWM used the spectral transform method for the evaluation of all nonlinear terms and local physical processes. Qualitatively, the numerical integration procedure steps through time in gridpoint space by an evaluation of all nonlinear terms on the Gaussian grid, forward transformation via a Fast Fourier Transform and Gaussian quadrature of the nonlinear products from gridpoint space to spectral space where spatial derivatives are evaluated, computation of spectral coefficients of the prognostic variables at time  $t + \Delta t$  and an inverse transform of the spectral quantities to physical (gridpoint) space (Hack and Jakob, 1992).

In vector form, the horizontal momentum and mass continuity equations governing the behavior of the SSWM are written as

$$\frac{d\mathbf{V}}{dt} = -f \mathbf{k} \times \mathbf{V} - \nabla\Phi, \quad (1)$$

and

$$\frac{d\Phi}{dt} = -\Phi \nabla \cdot \mathbf{V}, \quad (2)$$

where  $\mathbf{V} = \mathbf{i}u + \mathbf{j}v$  is the horizontal vector velocity,  $\mathbf{i}$  and  $\mathbf{j}$  are the unit vectors in the eastward and northward directions respectively,  $\mathbf{k}$  is the vertical unit vector,  $f = 2\Omega \sin \phi$  is the Coriolis parameter,  $\nabla$  is the del or gradient operator,  $\Phi = gh$  is the free surface geopotential,  $g$  is the gravitational acceleration,  $h = \bar{H} + h'$  (where  $h' \ll \bar{H}$ ) is the depth of the fluid,  $\bar{H}$  is the equivalent depth,  $h'$  is a small surface perturbation,  $\Omega$  is the angular velocity of the earth, and  $\phi$  denotes latitude (Hack and Jakob, 1992).

The experiments performed with the SSWM involved the addition of a forcing function to simulate heating in the atmosphere. This forcing function involved the use of a forcing term in the continuity equation to produce heating. The mass continuity equation for shallow water flow is shown in equation (2). The heating function chosen for this model was based on the continuity equation because heating comes out in the continuity equation as follows:

$$\frac{d\Phi}{dt} + \Phi \nabla \cdot \mathbf{V} = \mathbf{M}, \quad (3)$$

where  $\mathbf{M}$  is a mass source and sink and is equivalent to heating in the atmosphere. This is how heating was incorporated into the model. This heating was forced using the following equation:

$$F_{\Phi} = -\alpha \zeta \bar{\Phi} + F_{\Phi} = \mathbf{M}, \quad (4)$$

where  $\alpha$  is the forcing scaling factor (negative to produce a mass sink),  $\zeta$  is the relative vorticity,  $\bar{\Phi} = g\bar{h}$  is the mean geopotential, and  $F_{\Phi}$  is the geopotential forcing. This forcing function represents the heating being applied to excite vorticity in the model. The premise under which this forcing is applied is as follows:

- 1) If in the northern hemisphere:

- a. If  $\xi > 0$ ,  $F_\Phi = -\alpha\xi\overline{\Phi} + F_\Phi$  (e.g. heating is applied)
  - b. If  $\xi < 0$ ,  $F_\Phi = 0$  (e.g. no heating is applied)
- 2) If in the southern hemisphere:
- a. If  $\xi > 0$ ,  $F_\Phi = 0$
  - b. If  $\xi < 0$ ,  $F_\Phi = -\alpha\xi\overline{\Phi} + F_\Phi$

In this study, the aim was to excite vorticity at low levels in the troposphere. In order to accomplish this, a Gaussian type damping function was applied to the initial zonal and meridional wind and geopotential height fields to decrease the variation of the height field in the north-south direction so that we could use a smaller mean geopotential height, in essence using a shallow depth. The Gaussian function was as follows:

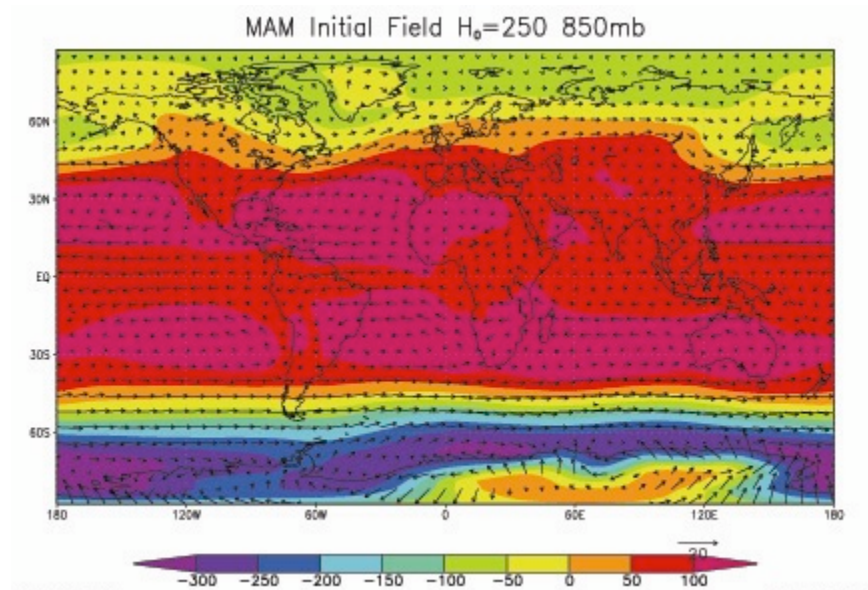
$$GAUS(i, j) = \exp\left(-0.0025(j - 30.5)^2\right), \quad (5)$$

where  $i$  and  $j$  are latitude and longitude points, respectively, on the grid. This Gaussian damping allowed for the initial mean geopotential,  $\overline{\Phi}_0$ , to be as low as  $250 \text{ m} \cdot g$  ( $g = 9.8 \text{ m/s}^2$ ).

We used 3 modifications of the realistic basic states in this study. Initially, the data was used to initialize the observational fields. The first modified basic state involved the use of the Gaussian damping function in equation (5). The second modified basic state was a zero basic state where all the observational fields, zonal wind, meridional wind, and geopotential height, were initialized to zero. The third modified basic state involved creating a simple basic state by averaging the initial observational fields along each latitude line, creating a zonally symmetric basic state. The initial, Gaussian damping, and zonally symmetric basic state initial fields at 850 mb are shown in Figures 3.1-3.6 for March-April-May (MAM), June-July-August (JJA), and

September-October (SO). The vectors represent the zonal and meridional winds and the shading represents the geopotential height field.

a)



b)

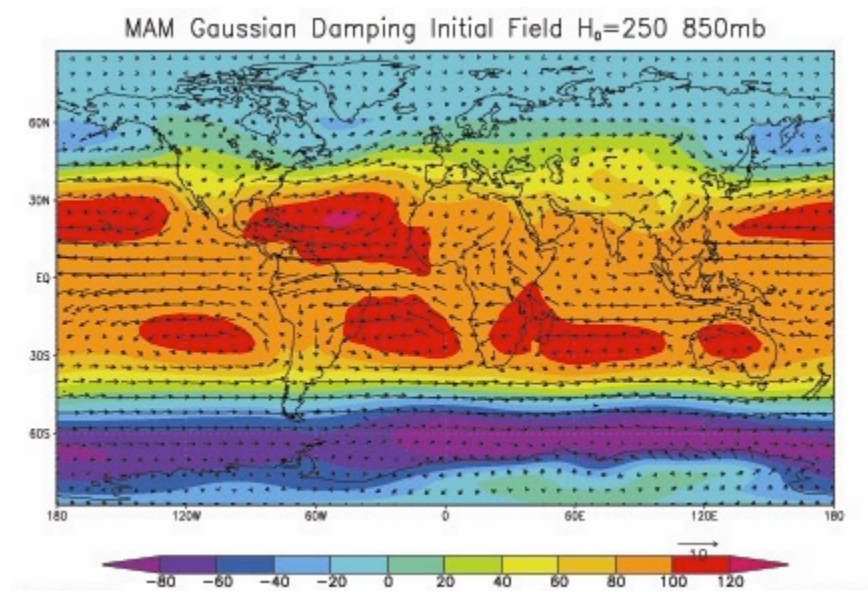
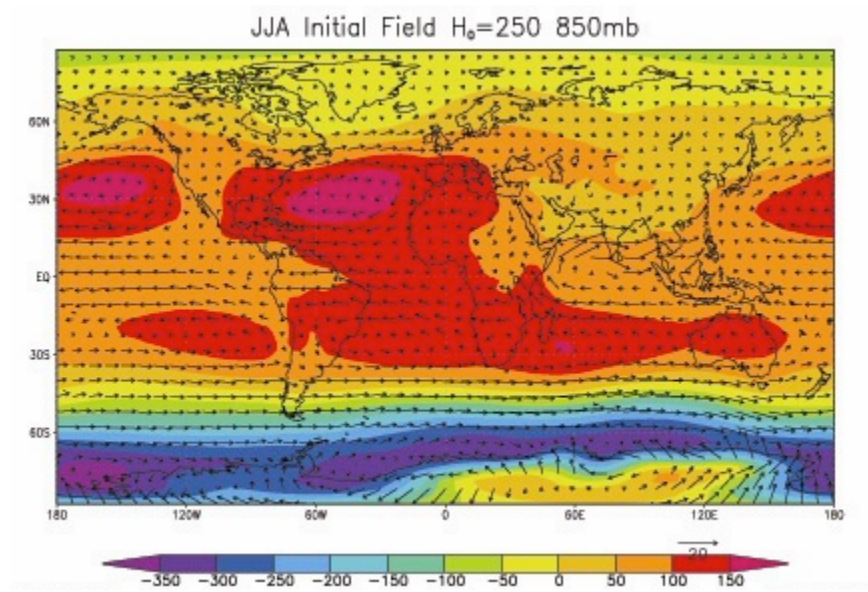


Figure 3.1 MAM a) initial and b) Gaussian damping initial field

a)



b)

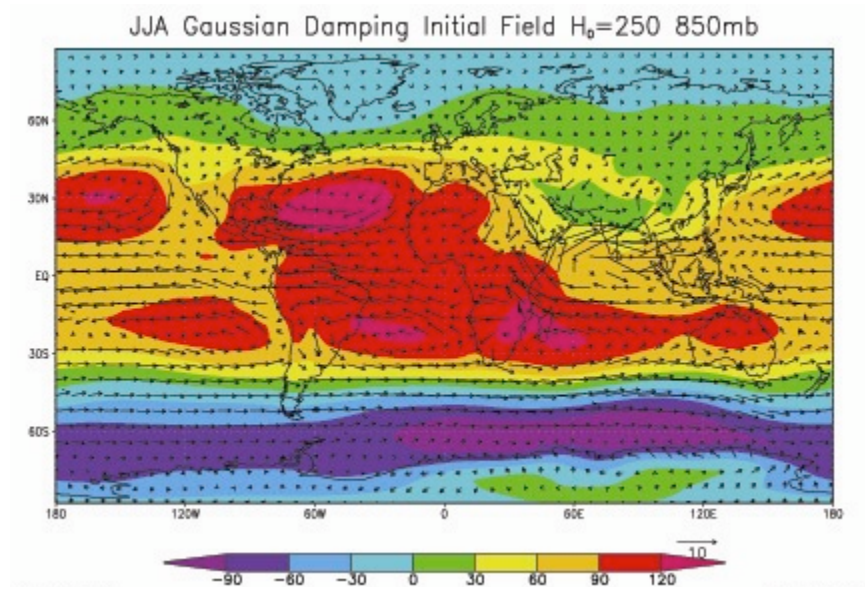
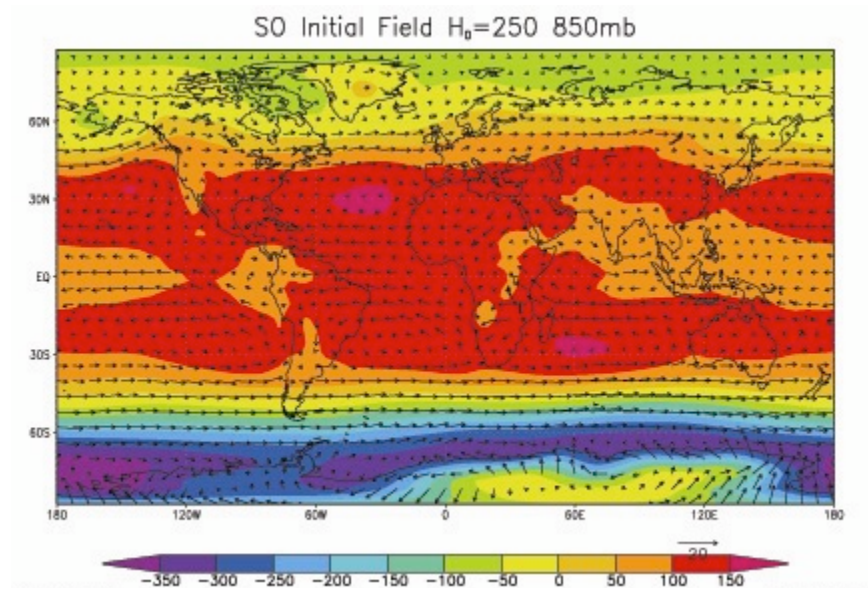


Figure 3.2 JJA a) initial and b) Gaussian damping initial field



a)



b)

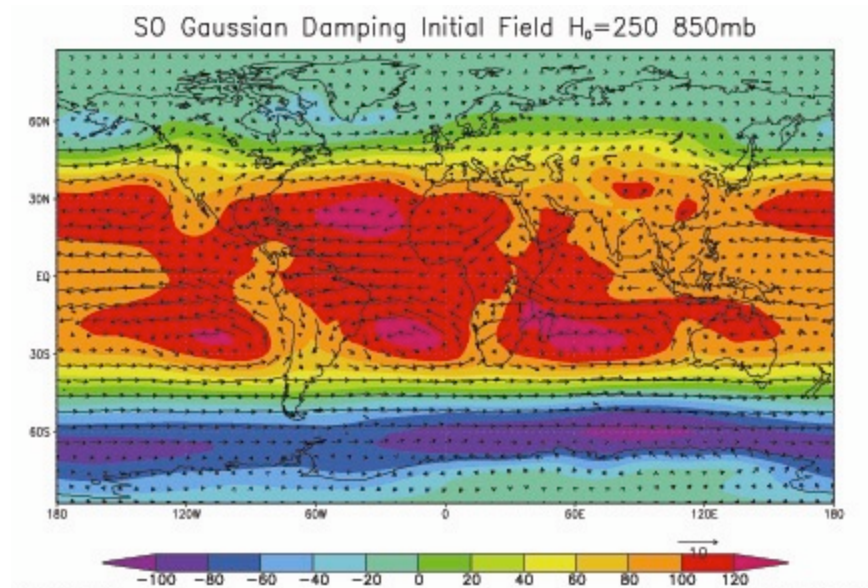


Figure 3.3 SO a) initial and b) Gaussian damping initial field



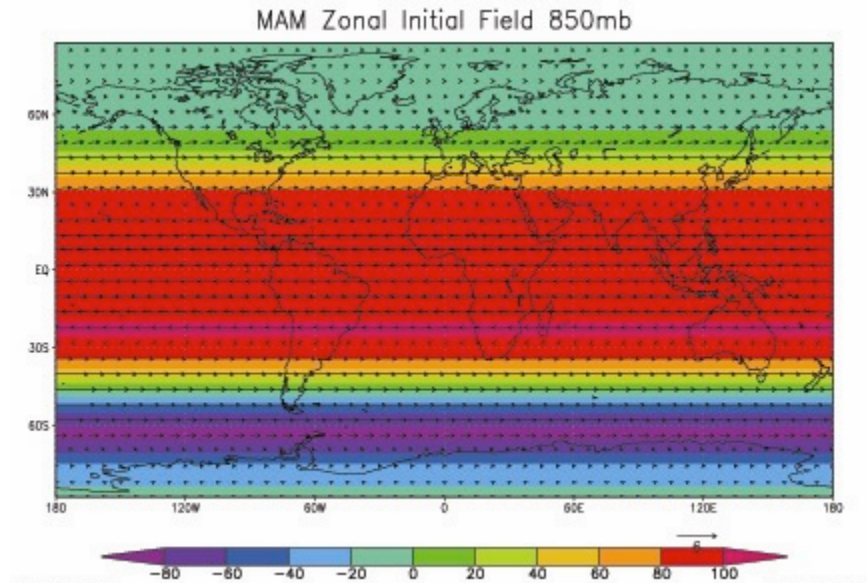


Figure 3.4 MAM zonal initial field

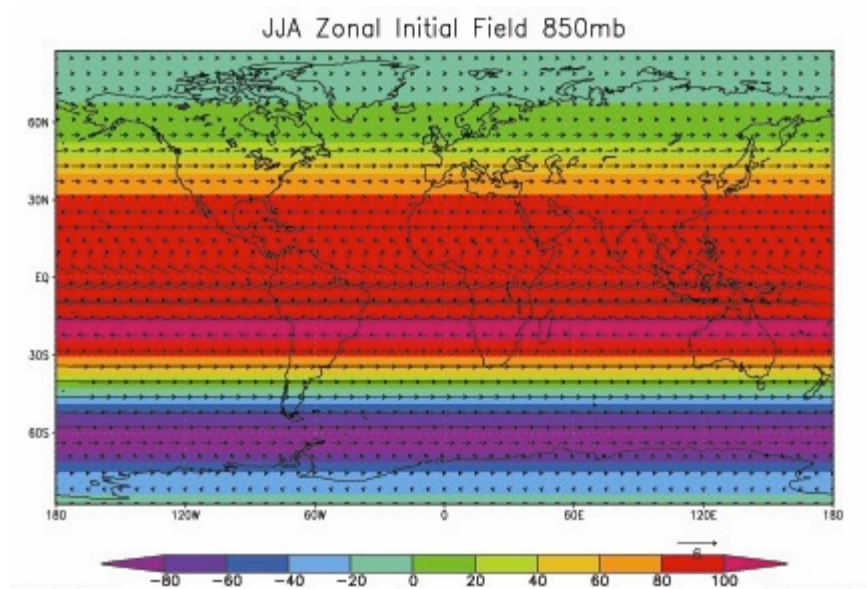


Figure 3.5 JJA zonal initial field

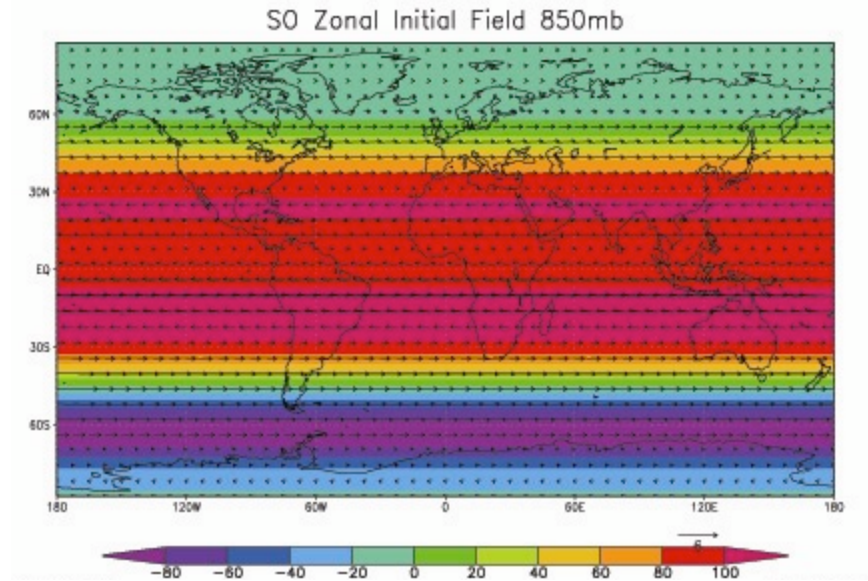


Figure 3.6 SO zonal initial field

Each model simulation began by initializing the model with the NCEP data. The parameters set for each simulation were the amplitude of the forcing,  $-12,500\text{m}^2/\text{s}^3$ , the initial depth of the heating, 250 m, and the length of time of the forcing, 120 hours (5 days). The model simulation time was 600 hours (25 days). The source region for the forcing was at  $40^\circ\text{E}$  and  $10^\circ\text{N}$ .

For each simulation, a basic state or a combination of basic states was chosen, Gaussian damping with a zonally symmetric initial field for example, to see the effects of Gaussian damping and different basic states on the observational fields (zonal and meridional wind and geopotential height) in the tropical region. The Gaussian damping was analyzed to see if there was a reduction in variation of the height and wind fields near the poles to allow for the response to be concentrated in the tropics. For each simulation, once a basic state was specified, the heating forcing function was applied with different scaling factors to see the effects of heating on

the height and wind fields. This response was analyzed to see how the change in the observational fields caused by heating creates a vorticity feedback. This vorticity feedback, associated with waves propagating outside of the forcing region and into energy wave accumulation zones, is believed to be a triggering mechanism for tropical cyclogenesis. To prevent the maximum vorticity feedback from existing in the forcing region, the forcing region was extended so that the latitude was between  $5^{\circ}$  N and  $15^{\circ}$  N and the longitude was  $\pm 10^{\circ}$  from  $40^{\circ}$  E. This created a larger non-feedback region in the forcing area and allowed a feedback region to exist outside the forcing area, which is the area of most interest.

Figure 3.7 shows the mean zonal wind field at 850 mb during September from 1968-1996. This figure shows a maximum easterly flow to the west of the African coast. Between  $10^{\circ}$  and  $25^{\circ}$  N, there is an initial increase then decrease in easterlies extending to the Windward Islands with an increase further westward. An energy wave accumulation region exists in the easterlies from  $50^{\circ}$  W to  $80^{\circ}$  W. There is a strong relationship between this accumulation region and tropical cyclone formation (from a spin up of vorticity).

The experiments conducted in this study investigated the response of different basic states to the heating forcing function in the forcing region and the cyclonic vorticity generated that enhances this heating in the atmosphere.

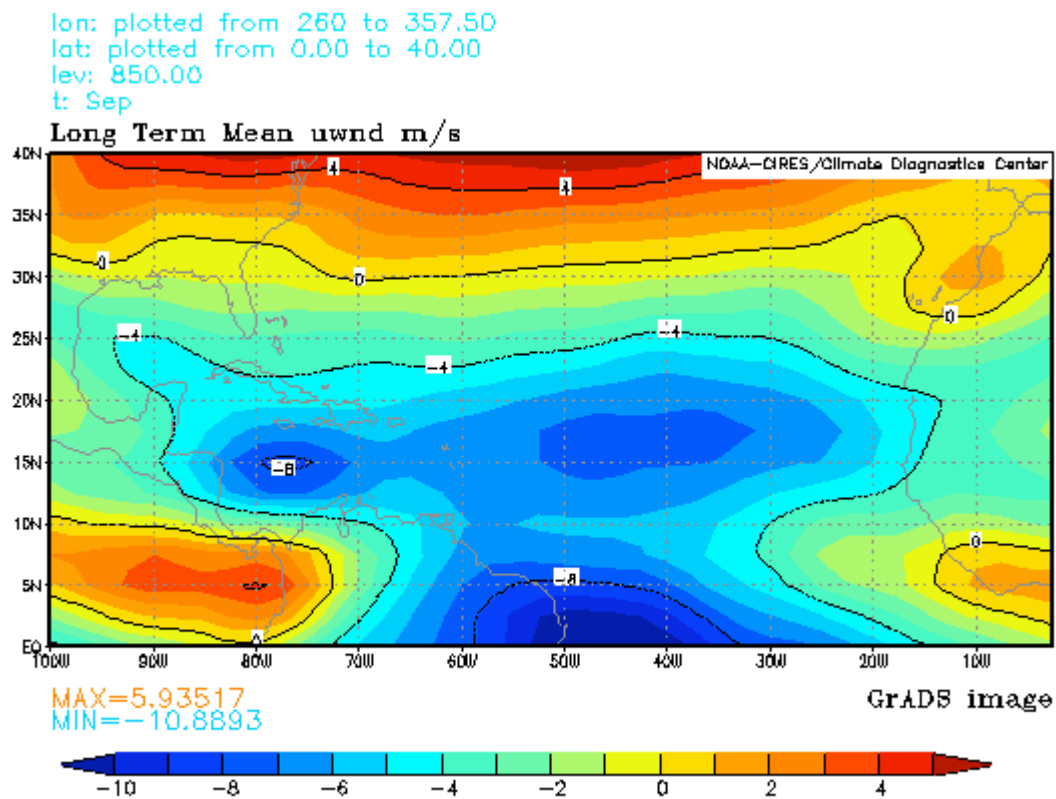


Figure 3.7 Mean zonal wind at 850 mb during September (Kalnay et al., 1996)

## CHAPTER 4

### RESULTS AND DISCUSSION

The results presented here will show how atmospheric heating creates a vorticity feedback mechanism. In cyclonic regions heating is enhanced and this in turn increases cyclonic vorticity in these regions, further enhancing heating and creating a vorticity feedback mechanism. Two different basic states will be shown to demonstrate the effects of heating and vorticity feedback. A zero basic state is used to compare the feedback effect in a pure wave propagation field. A zonally symmetric basic state will be shown because it is an example of a first approximation to the realistic basic state. Figures 3.3b and 3.6 show the realistic basic state and a zonally symmetric basic state initial field. The zonal and meridional wind fields in the tropics in parts of the Atlantic Ocean region in the zonally symmetric field are very similar to that of the realistic basic state and, therefore, will be used to represent a first approximation to the realistic basic state.

The area of most interest is the response in the tropics. In order to damp out the response at higher latitudes and allow the response to be concentrated in the tropics, a Gaussian damping function was applied to the initial zonally symmetric and realistic basic states. Before the addition of the Gaussian damping, the model could only be run at a depth as shallow as 500 m. Figures 4.1-4.4 show the zonal (U) and meridional (V) wind and height (H) fields with and without Gaussian damping. Once Gaussian damping was applied, the model was able to run at a depth as shallow as 250 m. The addition of Gaussian damping increased the stability of the model at this shallow depth so that it could run for the entire 600 hours of the simulation. The

Gaussian damping also damped out the height and wind fields at the poles so that the response could be concentrated in the tropical region.

The zonally symmetric basic state helped to make the field uniform along each latitude line. Using this basic state allowed us to view how a zonally symmetric basic state (as an approximation to the realistic basic state) affects the initial UVH fields and how cyclonic vorticity enhances heating in the atmosphere with a simple zonally symmetric flow. The enhanced heating can be seen in areas where the height field is lowered and the winds are stronger, indicating stronger cyclonic vorticity. For the zonally symmetric basic state simulation, the model was initialized with data that was averaged along each latitude line to create a non-varying, zonal basic state. Gaussian damping was applied to the initial UVH fields to concentrate the response in the tropics. The test case used set  $\alpha = -0.07$  in the heating forcing function to create a mass sink to simulate heating.

The zero basic state initialized the UVH field to zero. Using this basic state allowed us to view how a zero basic state affects the way UVH fields develop and respond to heating and how cyclonic vorticity enhances heating in the atmosphere with a zero basic state. The enhanced heating can be seen in areas where the height field is lowered and the winds are stronger. The test case used set  $\alpha = -0.07$  in the heating forcing function to create a mass sink to simulate heating.

#### 4.1 Effects of Gaussian Damping

The initial fields (Figures 3.1-3.3) show a significant difference once the Gaussian damping is applied. In MAM, before damping, the heights range from 0 to -100 m at the higher latitudes (near the poles) and are as high, in magnitude, as -300 m at lower latitudes (near the

poles). In the tropical region, the heights range from 50 to 100 m. The winds at the latitudes near the poles are as high as 20 m/s. Once damping is applied, the heights near the poles are less than half the magnitude they were previously and the winds are also damped. The Gaussian damping causes an increase in the height field in the tropical region, with a range of 80 to 100 m.

In JJA, before damping, the heights range from 0 to -100 m, -350 m, and from 50 to 150 m near the North and South Poles and in the tropical region, respectively. The winds at the latitudes near the poles are as high as 20 m/s. The Gaussian damping reduces the magnitude of the height field near the North Pole by a third, reduces the magnitude near the South Pole by almost 6 times, and significantly damps the winds near the poles. In the tropical region, the heights now range from 60 to 120 m.

In SO, the initial height fields are from 0 to -150 m and 0 to -350 m near the North and South Poles, respectively, and 50 to 150 m in the equatorial region. The winds at the latitudes near the poles are as high as 20 m/s. With the addition of Gaussian damping, heights near the North Pole are reduced by 7.5 times, heights near the South Pole are reduced by almost 6 times, and in the tropics now range from 80 to 120 m. Gaussian damping causes a reduction in the winds toward the poles.

## 4.2 Effect of Vorticity Feedback

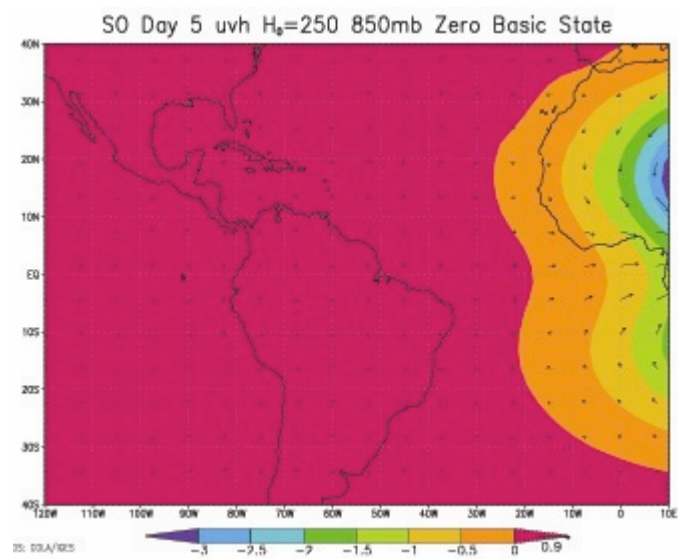
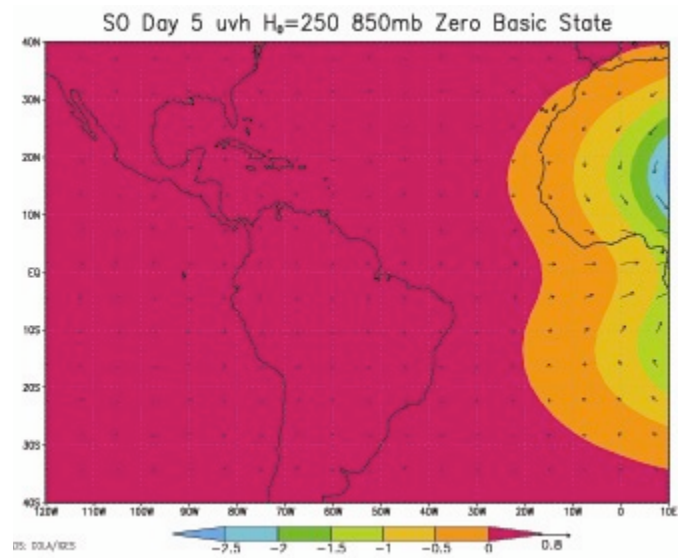
For each basic state, the heating forcing function was applied. The forcing function was scaled with different values of  $\alpha$  to create a mass sink. The cases shown here will represent heating with  $\alpha = -0.07$ . Other scaling factors were tested and it was determined that the larger the  $\alpha$  the stronger the heating response, and the smaller the  $\alpha$ , the weaker the heating response.

The zero basic state will show that in a pure wave propagation field, cyclonic vorticity enhances heating and creates a vorticity feedback mechanism. The zonally symmetric basic state will also show that in a zonally symmetric field the cyclonic vorticity enhances heating and creates a vorticity feedback, while also affecting the propagation of the cyclonic wave outside of the forcing region. The vorticity feedback created by enhanced heating in cyclonic regions is concentrated in the region of the forcing at  $40^{\circ}\text{E}$  and  $10^{\circ}\text{N}$ . We are most interested in the feedback and wave propagation outside of this region. In order to create a larger non-feedback zone in the region of the forcing, so that the feedback would exist further outside of the forcing region, the forcing region was extended to  $\pm 10^{\circ}$  from  $40^{\circ}\text{E}$  and  $\pm 5^{\circ}$  from  $10^{\circ}\text{N}$ . The extension of the non-feedback region will show an increase in wave propagation outside of the forcing region.

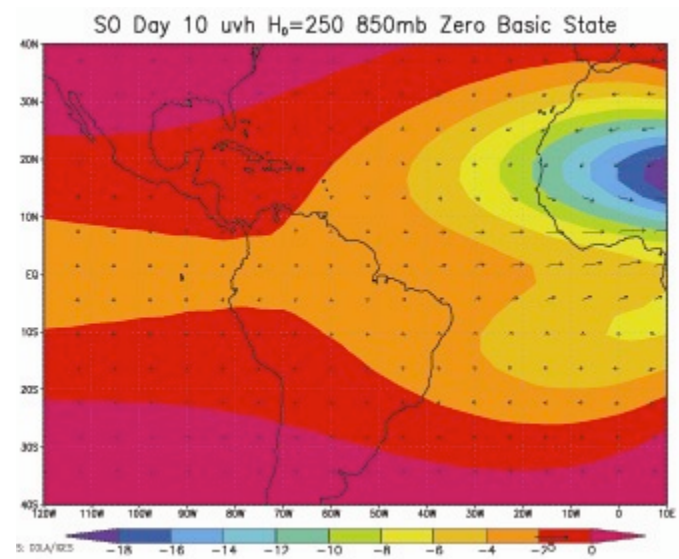
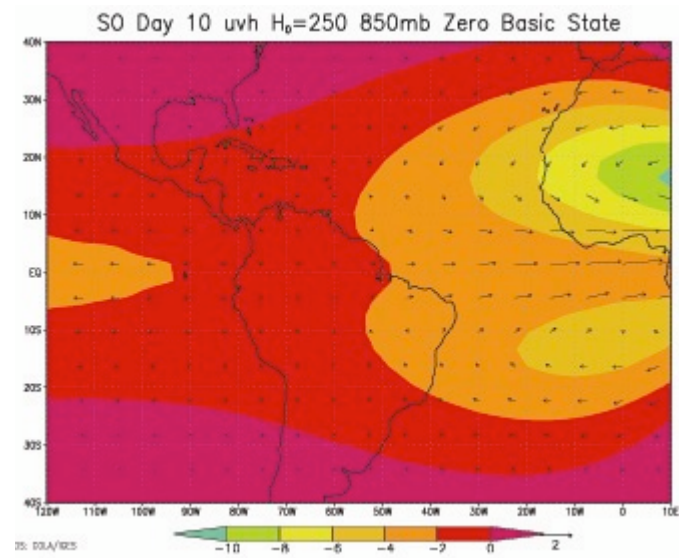
Figures 4.1 and 4.2 show the zero and zonally symmetric basic state UVH field for days 5, 10, 15, and 20 of the 25 day (600 hours) model simulation time. For each day, a case is shown comparing the basic state without heating and the basic state with heating to show the effects of the vorticity feedback mechanism. Figure 4.3 shows the case where the vorticity non-feedback region was extended for days 5, 10, 15, and 20 of the 25 day (600 hours) model simulation time.



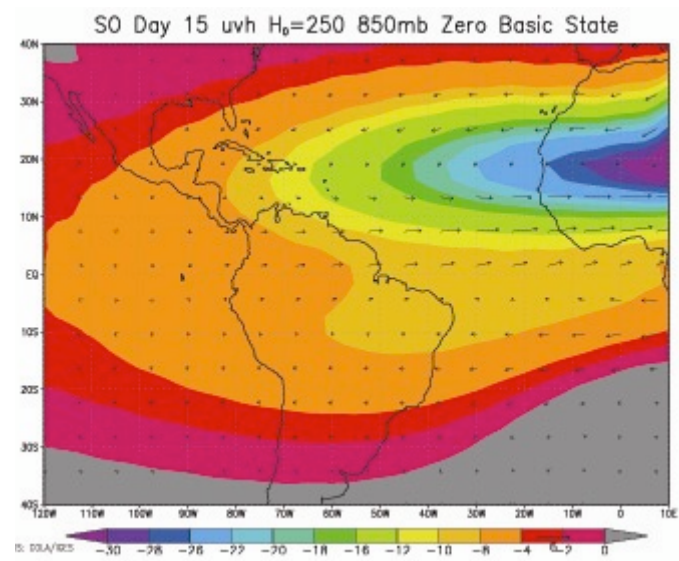
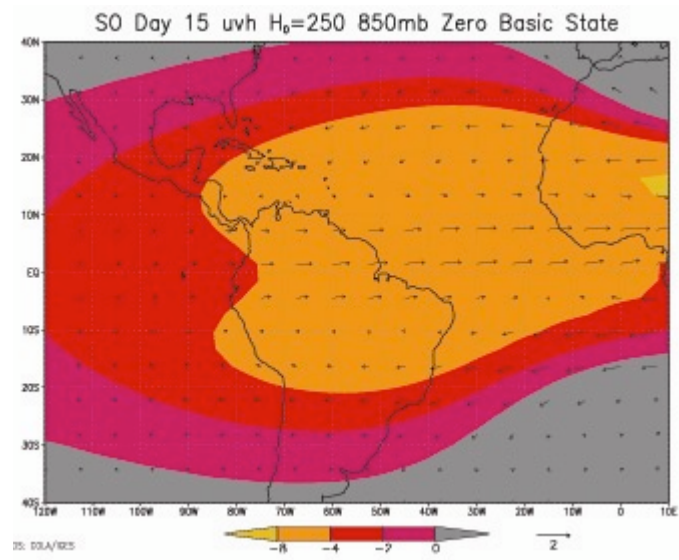
a) Zero Basic State Day 5



b) Zero Basic State Day 10



c) Zero Basic State Day 15



d) Zero Basic State Day 20

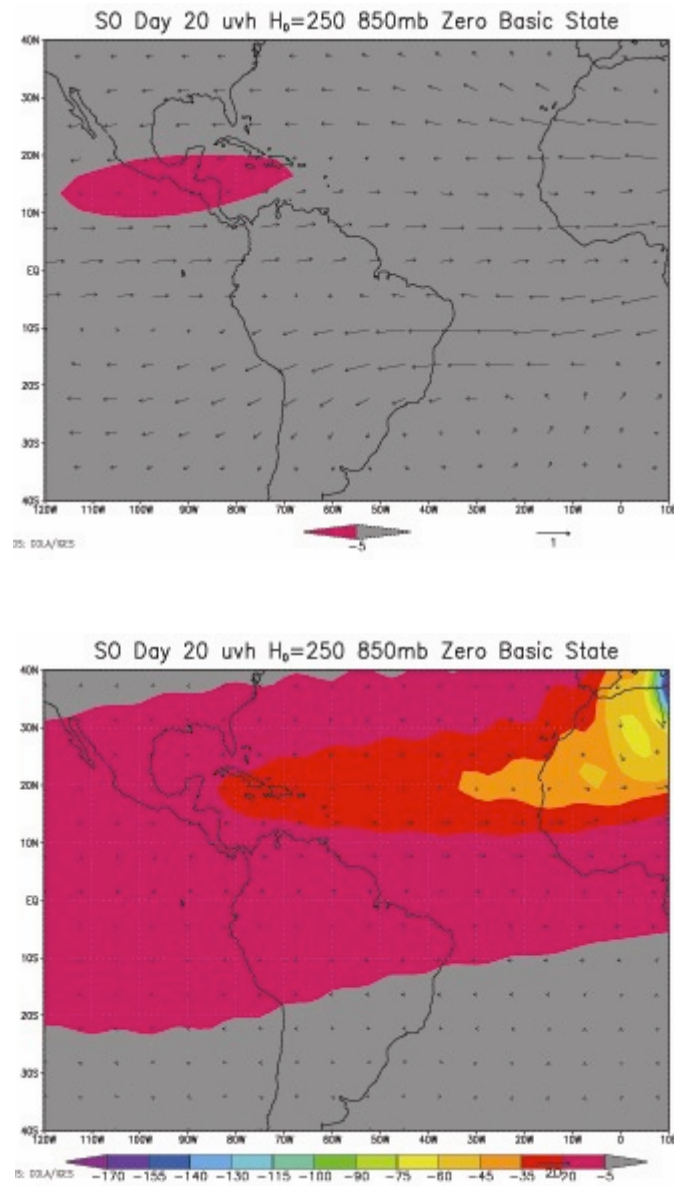
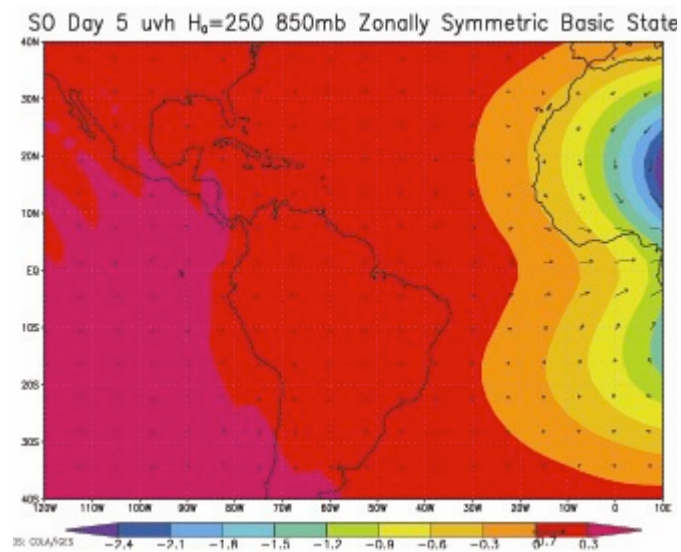
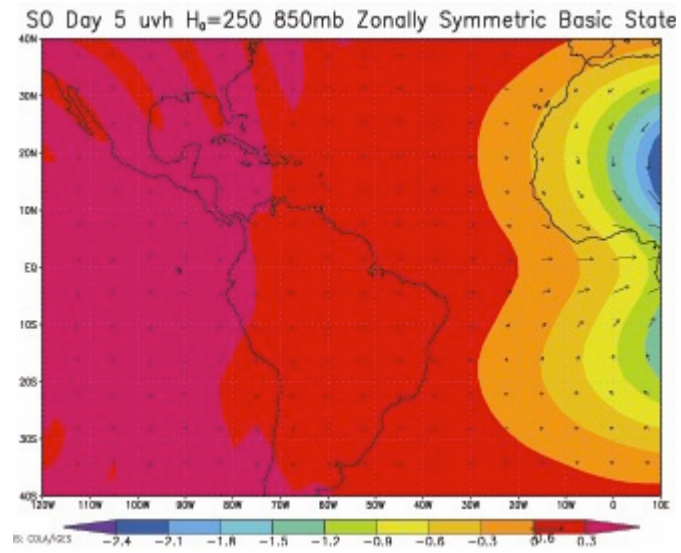


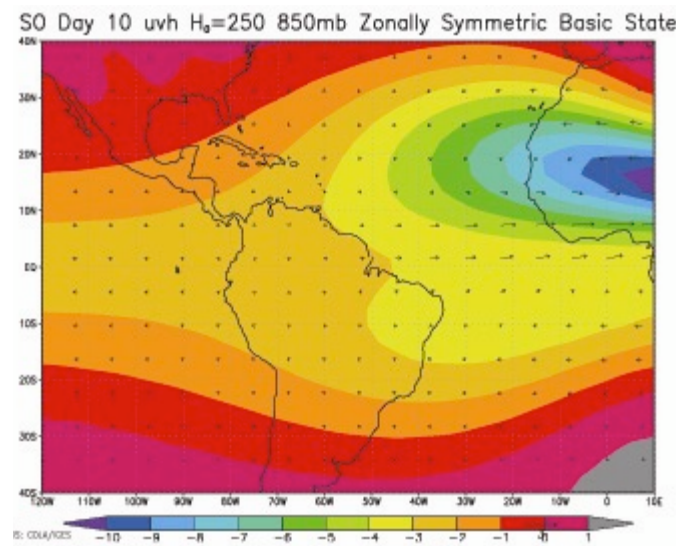
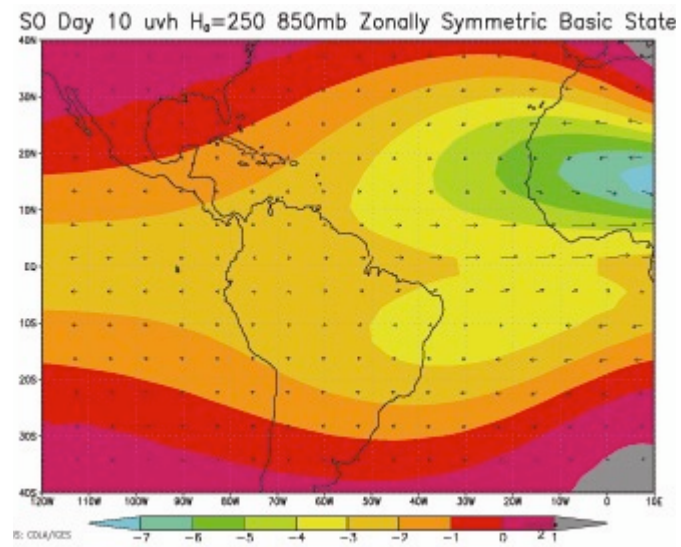
Figure 4.1 SO Zero basic state UVH field without heating (top panel) and with heating (bottom panel) at a) Day 5, b) Day 10, c) Day 15, and d) Day 20

a) Zonally Symmetric Basic State Day 5

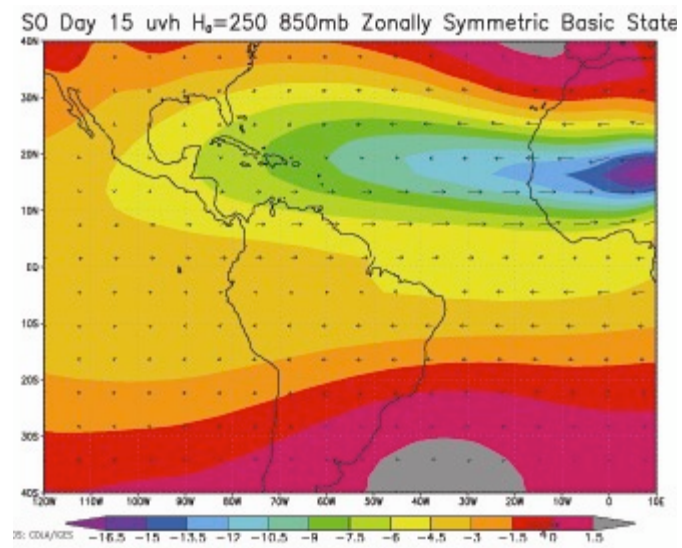
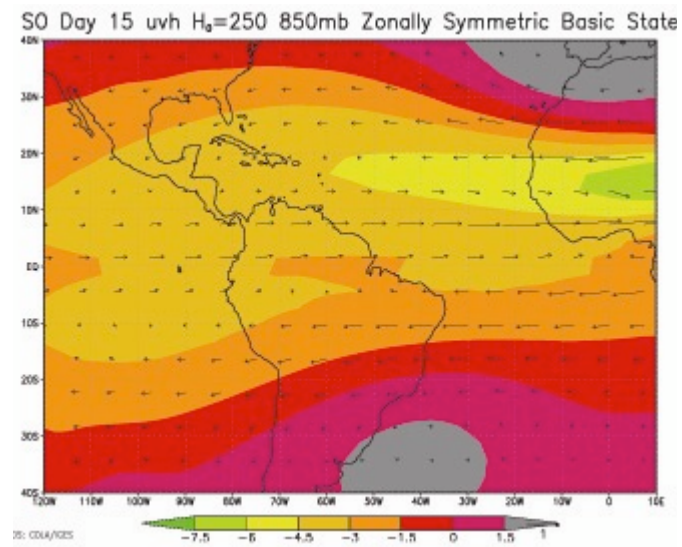




b) Zonally Symmetric Basic State Day 10



c) Zonally Symmetric Basic State Day 15



d) Zonally Symmetric Basic State Day 20

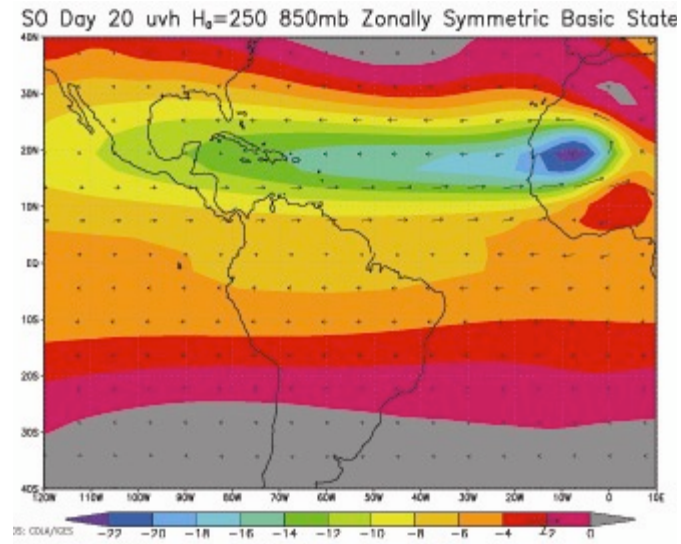
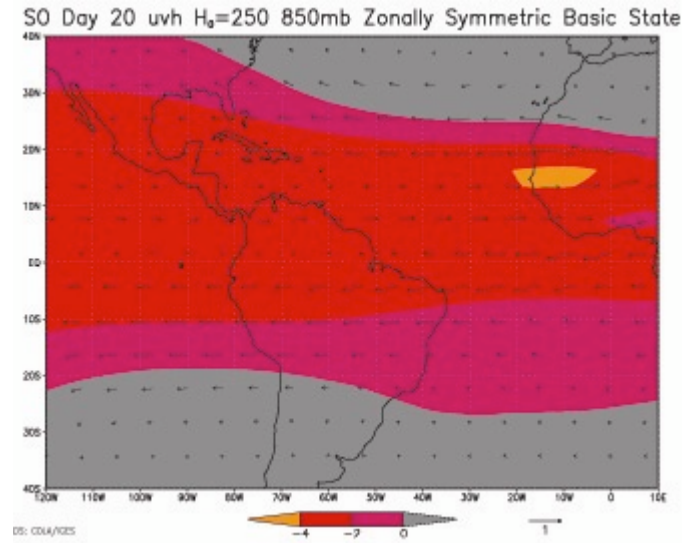
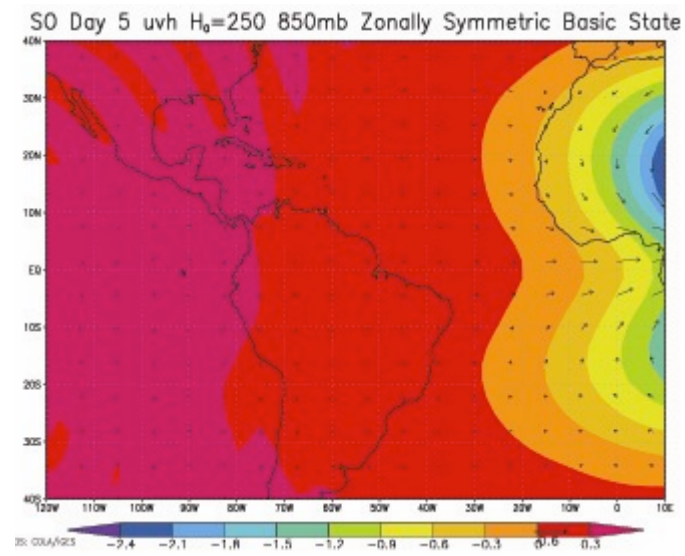


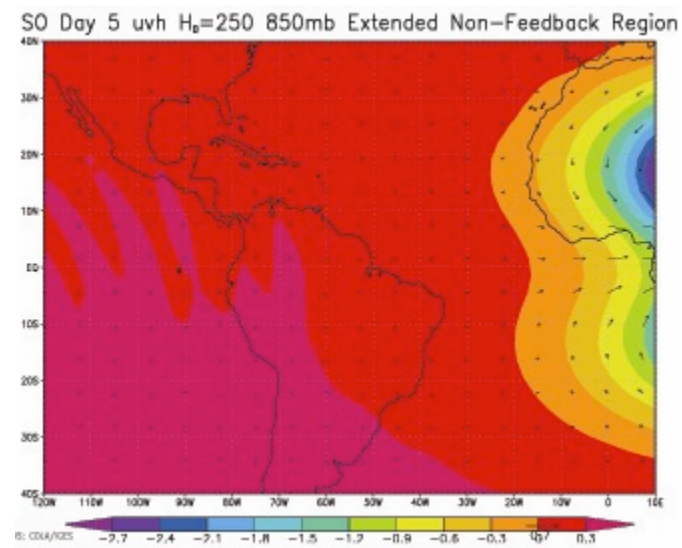
Figure 4.2 SO Zonally symmetric basic state UVH field without heating (top panel) and with heating (bottom panel) at a) Day 5, b) Day 10, c) Day 15, and d) Day 20



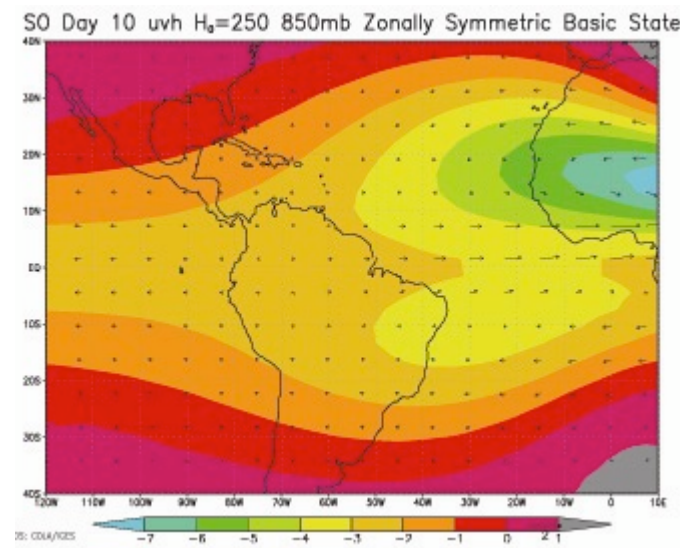
a) Zonally Symmetric Basic State Day 5



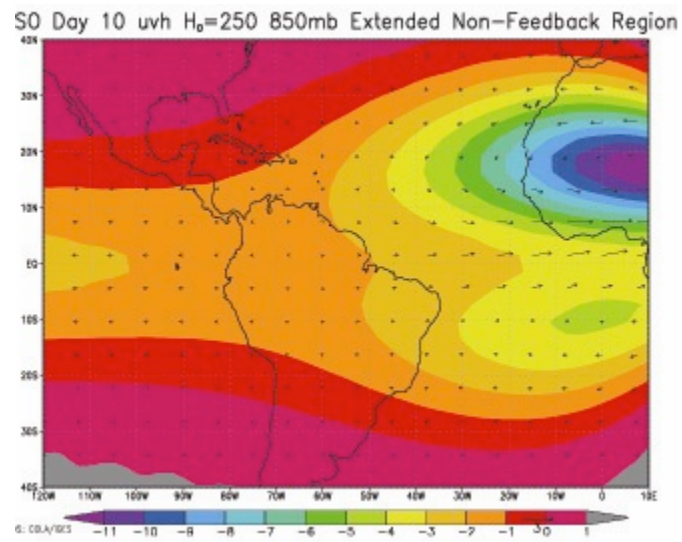
Extended Non-Feedback Region



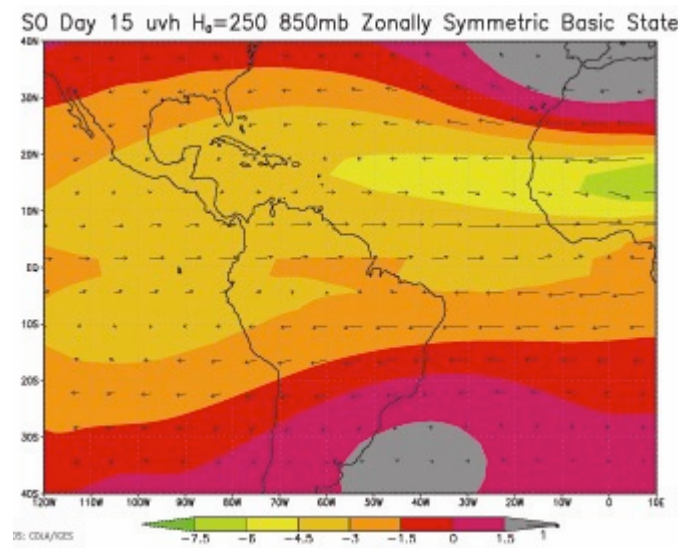
b) Zonally Symmetric Basic State Day 10



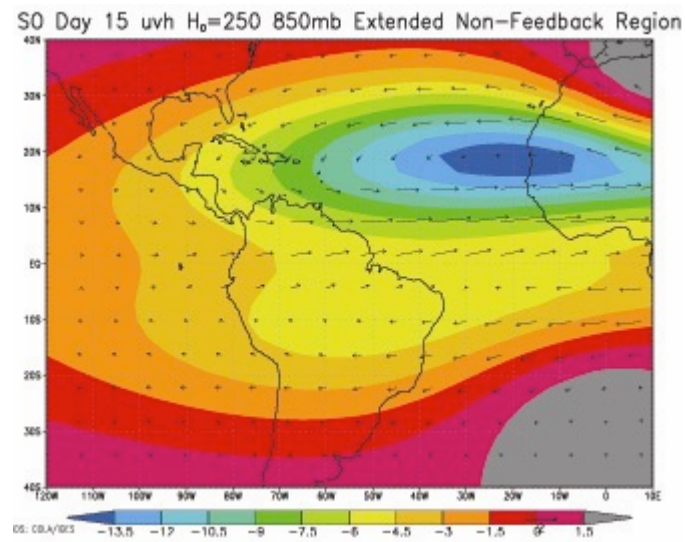
Extended Non-Feedback Region



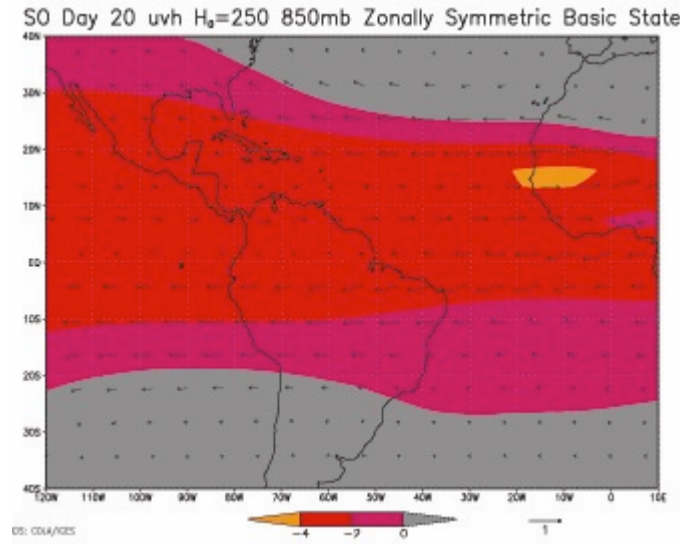
c) Zonally Symmetric Basic State Day 15



Extended Non-Feedback Region



d) Zonally Symmetric Basic State Day 20



Extended Non-Feedback Region

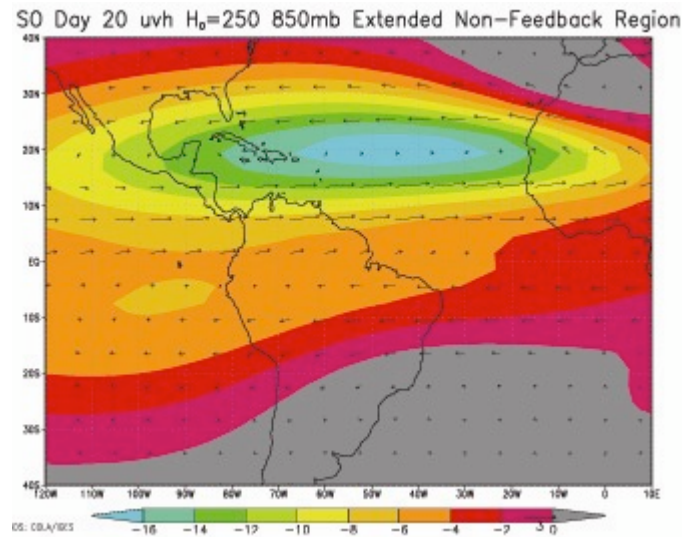


Figure 4.3 SO Zonally symmetric basic state UVH field without heating (top panel) and with heating and vorticity non-feedback region extended (bottom panel) at a) Day 5, b) Day 10, c) Day 15, and d) Day 20

### 4.3 Discussion

The heating in the model was proportional to cyclonic vorticity. An increase in cyclonic vorticity caused an increase in heating and produced a vorticity feedback mechanism. The scaling factor determined to be most effective in creating a mass sink without too much or too little feedback was  $\alpha = -0.07$ .

Applying Gaussian damping was effective in stabilizing the model so that it could run for the entire 600 hours at a depth of 250 m. It was also effective at damping the UVH field near the poles and concentrating the response in the tropical region.

With the zero basic state, initially, the magnitude of the response was very similar between the heating and non-heating cases. However, after 10 days, the zero basic state dramatically lowered the height field in the forcing region (by as much as 36 times) and also increased the strength of the winds in this area of stronger cyclonic vorticity. The zero basic state showed very little effect on the ability of the strong cyclonic wave to propagate westward outside of the forcing region.

With the zonally symmetric basic state, again early in the model simulation time, the height and wind fields are very similar between the heating and non-heating cases. At day 15, however, the magnitude of the height field is lowered by twice as much as the case without heating and by day 20 by almost 6 times. The zonally symmetric basic state was effective at lowering the height field and increasing winds, and also provided a mechanism for a small increase in westward propagation of the lowered height field and stronger winds.

At day 15, the lowered height field and stronger winds in the area of lowered heights, indicate that the extension of the vorticity non-feedback region in the zonally symmetric case with heating increases the strength of the cyclonic vorticity compared to the case without

heating. The extension of the vorticity non-feedback region also shows that this stronger cyclonic wave continues to intensify through day 20 and propagates westward into the Atlantic Ocean.

## CHAPTER 5

### CONCLUSION AND FUTURE WORK

This study has focused on the relationship between heating and cyclonic vorticity. The ultimate goal of this study was to find the optimal conditions, using a spectral shallow water model with a heating function, under which cyclonic vorticity enhances heating in the atmosphere. The model was limited by its inability to utilize sea surface temperatures and its inability to produce heating directly, as opposed to using a mass sink acting as a heating function.

The majority of the focus of this study was in SO since the response during this period was higher than JJA and the MAM case did not produce a significant response to the heating function. Since the region of the forcing was placed in the Northern Hemisphere, there was not a significant response in the Southern Hemisphere.

The zonally symmetric basic state with an extended vorticity non-feedback region proved to be the most effective at creating a vorticity feedback and increasing the propagation of the cyclonic wave westward into the Atlantic Ocean. The zero basic state created the most intense cyclonic wave, but since it was unable to propagate westward, these results are not desirable. The results of this study indicate that cyclonic vorticity does enhance heating in the atmosphere and produce a vorticity feedback.

Results of this study can be used to better understand the nonlinear feedback created when atmospheric heating is enhanced by cyclonic vorticity. The results can be applied to a realistic, zonally varying basic state to test how waves change scale in zones of negative

stretching deformation ( $\partial U/\partial x < 0$ ), how these waves accumulate with a finite  $\partial U/\partial x < 0$ , and if this leads to tropical cyclogenesis.



## REFERENCES

- Aiyyer, Anantha R., and John Molinari (2003). Evolution of Mixed Rossby–Gravity Waves in Idealized MJO Environments. *Journal of the Atmospheric Sciences*, Vol. 60, No. 23, 2837-2855.
- American Meteorological Society (2000). Glossary of Meteorology. Retrieved May 18, 2005 from <http://amsglossary.allenpress.com/glossary>
- Browning, G.L., J. J Hack, P. N. Swarztrauber (1989). A Comparison of Three Numerical Methods for Solving Differential Equations on the Sphere. *Monthly Weather Review*, 117, 1058-1075.
- Chang, Hai-Ru, Peter J. Webster (1990). Energy Accumulation and Emanation at Low Latitudes. Part II: Nonlinear Response to Strong Episodic Equatorial Forcing. *Journal of the Atmospheric Sciences*, 47, 2624-2644.
- Chang, Hai-Ru, and Peter J. Webster (1995). Energy Accumulation and Emanation at Low Latitudes. Part III: Forward and Backward Accumulation. *Journal of the Atmospheric Sciences*, 52, 2384-2403.
- Charney, Jule G., Arnt Eliassen (1964). On the Growth of the Hurricane Depression. *Journal of the Atmospheric Sciences*, 21, 68-75.
- Dickinson, Michael, Molinari, John (2002). Mixed Rossby–Gravity Waves and Western Pacific Tropical Cyclogenesis. Part I: Synoptic Evolution. *Journal of the Atmospheric Sciences*, 59, 2183-2196.
- Eliassen E. B. Machenhauer, and E. Rasmussen (1970). On a Numerical Method for Integration of the Hydrodynamical Equations with a Spectral Representation of the Horizontal Fields. Report No. 2, Institut for Teoretisk Meteorologi, University of Copenhagen.
- Emanuel, Kerry A. (1986). An Air-Sea Interaction Theory for Tropical Cyclones. Part I: Steady State Maintenance. *Journal of the Atmospheric Sciences*, 43, 585-604.
- Emanuel, Kerry A. (1991). The Theory of Hurricanes. *Annual Review of Fluid Mechanics*, Vol. 23, 179-196.
- Ferreira, R. N., and J. J. Hack (1996). Dynamical Aspects of Twin Tropical Cyclones Associated with the Madden–Julian Oscillation. *Journal of the Atmospheric Sciences*, 53, 929–945.

- Gray, W. (1979). Hurricanes: Their Formation, Structure, and Likely Role in the Tropical Circulation. *Meteorology over the Tropical Oceans*, D. B. Shaw, Ed., Royal Meteorological Society, 155–218.
- Hack, James J., and Ruediger Jakob (1992). Description of a Global Shallow Water Model Based on the Spectral Transform Method. NCAR Technical Note NCAR/TN-343+STR, National Center for Atmospheric Research, 39 pp.
- Kalnay, E., M. Kanamitsu, R. Kistler, W. Collins, D. Deaven, L. Gandin, M. Iredell, S. Saha, G. White, J. Woollen, Y. Zhu, A. Leetmaa, B. Reynolds, M. Chelliah, W. Ebisuzaki, W. Higgins, J. Janowiak, K.C. Mo, C. Ropelewski, J. Wang, Roy Jenne, Dennis Joseph (1996). The NCEP/NCAR 40-Year Reanalysis Project. *Bulletin of the American Meteorological Society*, Vol. 77, No. 3, 437-472.
- Kleinschmidt, E. Jr. (1951). Grundlagen einer Theorie des tropischen Zyklonen. *Arch. Meteorol., Geophys. Bioklimatol., Ser. A* 4: 53-72.
- Lawrence, Mark G. (2004). Parameterizing Convection. Retrieved May 20, 2005 from [http://www.mpch-mainz.mpg.de/~lawrence/vorlesung\\_WS2004-5/parameterization.pdf](http://www.mpch-mainz.mpg.de/~lawrence/vorlesung_WS2004-5/parameterization.pdf).
- Liebmann, B., H. H. Hendon, and J. D. Glick (1994). The Relationship Between Tropical Cyclones of the Western Pacific and Indian Oceans and the Madden–Julian Oscillation. *Journal of the Meteorological Society of Japan*, 72, 401–411.
- Maloney, Eric D., Dennis L. Hartmann (2000). Modulation of Eastern North Pacific Hurricanes by the Madden–Julian Oscillation. *Journal of Climate* Vol. 13, No. 9, 1451-1460.
- Maloney, Eric D., Dennis L. Hartmann (2000). Modulation of Hurricane Activity in the Gulf of Mexico by the Madden-Julian Oscillation. Vol 287, 2002-2004.
- Matsuno, Taroh (1966). Quasi-Geostrophic Motions in the Equatorial Area. *Journal of the Meteorological Society of Japan*, 44, 25-43.
- Reed, R.J., A. Hollingsworth, W.A. Heckley, F. Delsol (1988). An Evaluation of the Performance of the ECMWF Operational System in Analyzing and Forecasting Easterly Wave Disturbances over Africa and the Tropical Atlantic. *Monthly Weather Review*, 116, 824-865.
- Riehl, H. 1954. *Tropical Meteorology*. New York: McGraw-Hill. 392 pp.
- Sobel, Adam H., Christopher S. Bretherton (1999). Development of Synoptic-Scale Disturbances over the Summertime Tropical Northwest Pacific. *Journal of the Atmospheric Sciences*, 56, 3106-3127.
- Sobel, A. H., and E. D. Maloney (2000). Effect of ENSO and the MJO on Western North Pacific Tropical Cyclones. *Geophysical Res. Lett.*, 27, 1739-1742.

- Thorncroft, C.D. and K.I. Hodges (2001). African Easterly Wave Variability and Its Relationship to Atlantic Tropical Cyclone Activity, *Journal of Climate*, 14, 1166-1179.
- Webster, Peter J., G. Holland, B. Houze (2005). Wave Accumulation in the Equatorial Duct and Tropical Cyclone Genesis, 85<sup>th</sup> American Meteorological Society Annual Meeting.
- Webster, Peter J., Hai-Ru Chang (1988). Equatorial Energy Accumulation and Emanation Regions: Impacts of a Zonally Varying Basic State. *Journal of the Atmospheric Sciences*, 45, 803-829.
- Webster, Peter J., James R. Holton (1982). Cross-Equatorial Response to Middle-Latitude Forcing in a Zonally Varying Basic State. *Journal of the Atmospheric Sciences*, 39, 722-733.
- Williamson, David L., John B. Drake, James J. Hack, Rüdiger Jakob, Paul N. Swarztrauber (1992). A Standard Test Set for Numerical Approximations to the Shallow Water Equations in Spherical Geometry. *Journal of Computational Physics*, Volume 101, Issue 1, 227-228.
- Yamazaki, N., and M. Murakami (1989). An Intraseasonal Amplitude Modulation of the Short-Term Tropical Disturbances over the Western Pacific. *Journal of the Meteorological Society of Japan*, 67, 791–807.